ISSN 0915-633X

NATIONAL INSTITUTE FOR FUSION SCIENCE

Development of Computational Technique for Labeling Magnetic Flux-surfaces

M. Nunami, R. Kanno, S. Satake, H. Takamaru and T. Hayashi

(Received - Feb. 22, 2006)

NIFS-831

Mar. 2006

RESEARCH REPORT
NIFS Series

TOKI, JAPAN

Development of computational technique for labeling magnetic flux-surfaces

Masanori NUNAMI[1)], Ryutaro KANNO[1)], Shinsuke SATAKE[1)], Hisanori TAKAMARU[2)] and Takaya HAYASHI[1),3)]

[1)] *National Institute for Fusion Science, Toki 509-5292, Japan*
[2)] *Department of Computer Science, Chubu University, Kasugai 487-8501, Japan*
[3)] *Department of Fusion Science, Graduate University for Advanced Studies, Toki 509-5292, Japan*

In recent Large Helical Device (LHD) experiments, radial profiles of ion temperature, electric field, etc. are measured in the $m/n = 1/1$ magnetic island produced by island control coils, where m is the poloidal mode number and n the toroidal mode number. When the transport of the plasma in the radial profiles is numerically analyzed, an average over a magnetic flux-surface in the island is a very useful concept to understand the transport. On averaging, a proper labeling of the flux-surfaces is necessary. In general, it is not easy to label the flux-surfaces in the magnetic field with the island, compared with the case of a magnetic field configuration having nested flux-surfaces. In the present paper, we have developed a new computational technique to label the magnetic flux-surfaces. This technique is constructed by using an optimization algorithm, which is known as an optimization method called the *simulated annealing method*. The flux-surfaces are discerned by using two labels: one is classification of the magnetic field structure, i.e., core, island, ergodic, and outside regions, and the other is a value of the toroidal magnetic flux. We have applied the technique to an LHD configuration with the $m/n = 1/1$ island, and successfully obtained the discrimination of the magnetic field structure.

Keywords: Large Helical Device, magnetic island, flux-surface, Poincaré plots, annealing method

1 Introduction

A flux-surface average of some quantity, e.g., particle flux, heat flux, etc., is a very useful concept for transport analysis of a toroidal plasma. The flux-surface average of a function $\Phi(\boldsymbol{x})$ is defined by the volume average over an infinitesimally small shell with volume ΔV, where ΔV lies between two neighboring flux-surfaces with volumes V and $V + \Delta V$, and is denoted as

$$\langle \Phi(\boldsymbol{x}) \rangle := \lim_{\Delta V \to 0} \frac{1}{\Delta V} \iiint_{\Delta V} \Phi(\boldsymbol{x}) d^3x, \qquad (1)$$

if there exist the closed flux-surfaces. On averaging, we have to label the magnetic flux-surfaces, e.g., if the nested flux-surfaces exist, the surface is labeled as the volume enclosed by the surface in the Hamada coordinates [1], and as the toroidal magnetic flux in the Boozer coordinates [2,3]. In a non-axisymmetric configuration, the existence of nested flux-surfaces is not guaranteed [4]. However, it is possible to numerically obtain an MHD equilibrium having closed magnetic surfaces by using a suitable three dimensional equilibrium code which does not assume the existence of nested flux-surfaces, e.g., HINT code [5–7]. In general, such an equilibrium includes magnetic islands and ergodic regions. Thus, it is not easy to label the magnetic surfaces. Without any approximations, we cannot evaluate the flux-surface averages in terms of magnetic coordinates in a non-axisymmetric configuration. Although quasi magnetic-coordinates can be constructed on the equilibrium with the islands as shown in Refs. [8–12], the coordinate system does not correspond to a magnetic coordinate system along the flux-surfaces in the islands.

In recent Large Helical Device (LHD) experiments, radial profiles of ion temperature, electric field, etc. are measured in the $m/n = 1/1$ magnetic island produced by island control coils [13, 14]. The numerical transport analysis is required for understanding the experimental results, thus the average over a flux-surface of the island is necessary.

In the present paper, we develop a new computational technique for labeling magnetic surfaces in the LHD configuration. The flux-surfaces can be basically labeled by tracing field lines, as shown in Refs. [15–18]. The main task of the technique is to identify a flux-surface from the Poincaré plots of a field line on a poloidal cross section. For the identification, the points of the Poincaré plots, i.e., the Poincaré points, should be numbered along a closed curve given from the poloidal cross section of a flux-surface, where this procedure is called the *ordering* of the Poincaré points in this paper. One of the simplest methods ordering the Poincaré points is to search the nearest neighbor point of each point. However, this method often fails at, for example, a closed magnetic surface in the island. In order to improve the ordering procedure, we

author's e-mail: nunami.masanori@nifs.ac.jp

employ the algorithm which is a technique called the *simulated annealing method* [19, 20]. This method is familiar as a successful algorithm to solve the *traveling salesman problem* [21], which is the problem for a traveling salesman who has to visit a number of cities, how to plan the trip so that every city is visited once and just once and the whole trip is as short as possible. This method is useful for solving our problem, i.e., how to connect each Poincaré point of a field line. In the technique developed here, the magnetic flux-surfaces are identified by two labels, `IREGION` and `TFLUX`, which describe classification of magnetic field structure and a toroidal magnetic flux, respectively.

When the number of sampling flux-surfaces is quite large, the calculation code which is based on the developed technique should be parallelized. The code has been programed with the High Performance FORTRAN [22] on a vector parallel supercomputer.

This paper is organized as follows. In Sec.2, we show the outline of the developed technique which is constructed from three parts shown in subsections 2.1-2.3, and the numerical results are shown in subsection 2.4. Finally, a summary is given in Sec.3.

2 Computational Technique

We explain the outline of the technique hereafter. Figure 1 is the flowchart of the developed technique. As shown in the flowchart, the technique is constructed from three parts: I) Classification of regions, II) Ordering Poincaré points, and III) Calculation of toroidal magnetic flux. In the part I, for a given magnetic field configuration, we classify regions of the magnetic field structure, i.e., core, island, ergodic, and outside regions. In the part II, we trace a field line to obtain the Poincaré points on a poloidal cross section, and order these points by using two methods explained in Sec.2.2. In the part III, we calculate a value of the toroidal magnetic flux for the closed magnetic flux-surface given by the points, and label it by the value. In the following, we explain each part in detail.

2.1 Classification of regions

In this section, we consider the classification of regions of the magnetic field structure. Because there does not exist a magnetic coordinate system along the closed magnetic surfaces in both core and island regions, we have to classify the regions, as shown in Fig.2. We can discern four parts of the structure, i.e., outside, ergodic, island, and core regions. Here, we consider that the island is visible under certain numerical accuracy. Similarly, the ergodic region is considered to be visible, but be narrow.

First, we roughly evaluate an initial guess of the boundary between each region, and calculate several magnetic flux-surfaces near the initial guess. Then the suitable boundaries are determined by using the above flux-surfaces, if the ordering of the Poincaré points representing the flux-surfaces succeeds. By using the boundaries, we label the regions into four parts; `IREGION` = `1` (outside region), `2` (ergodic region), `3` (island region), and `4` (core region), as shown in Fig.2.

2.2 Ordering Poincaré points with annealing method

Next, we have to order the Poincaré points of a field line on a poloidal cross section, in order to identify a closed magnetic flux-surface. Note that in an ergodic region, a visible flux-surface does not exist, thus the field line tracing is not carried out in the region. For the ordering, we use two methods. One is the simple method ordering the points by searching the nearest neighbor point for each point, where the ordering begins from a given starting point of the Poincaré points. This is one of simple ways of ordering the points. But we frequently encounter a case that the simple method does not work well, as will see later. The other is based on the *simulated annealing method* [19,20]. This method is a famous optimization algorithm employed in the *traveling salesman problem* [21] (the problem of finding the shortest cyclical itinerary for a traveling salesman who must visit each of N cities in turn). We use it to order the Poincaré points, if the simple method does not work well; see the part II of Fig.1. In the following, we introduce a brief review of the simulated annealing method used for solving our problem.

2.2.1 Simulated annealing method

The simulated annealing method is a probabilistic algorithm for combinatorial optimization problems [23]. In particular, when a given function has many local extrema, the method is powerful to search the global extremum. Of course, the most sure method for searching the global extremum is to search for all possibilities; e.g., in the traveling salesman problem, the most sure method searches the true route with the minimum length from all possible routes. In such a method, we can always find the true extremum. But this method is extremely time-consuming; for example, in the traveling salesman problem to visit N cities, the calculation time increases as $\sim \exp(N)$ [23]. Note that the most sure method is completely different from the simple method explained above, because a starting point of searching the true route by the simple method is fixed. On the other hand, the simulated annealing method can give us a better solution under realistic calculation costs. Our main aim in this section is to identify a poloidal cross section of a flux-surface by using the Poincaré points of the field line. We assume that the cross section of the flux-surface is obtained by connecting the points with the shortest route. This assumption is not always guaranteed to identify the flux-surface, but it is almost valid for practical cases, as shown in Sec.2.2.3.

The simulated annealing method is formulated by the analogy with the annealing of a heated metal with lattice defects, under slowly cooling [19]. As the temperature decreases slowly, the heated metal forms the pure crystal which is the lowest energy state. On the other hand, if the temperature decreases rapidly, it forms the non-crystal which is not the lowest energy state. This analogy suggests us that the lowest state, i.e., the global minimum of its energy function, is obtained by cooling slowly. An energy equilibrium with a temperature T is distributed with a Boltzmann probability distribution,

$$P(E) \sim \exp\left(\frac{E}{kT}\right), \tag{2}$$

where k means the Boltzmann constant. According to the probability $P(E)$, a lower energy state can climb up to a higher energy state, i.e., there is a possibility that the system can escape from a local minimum of the energy to a better state. As shown in Fig.3, when the system is trapped in a local minimum of the function, it can escape from there with the probability $P \sim \exp[-(E_2 - E_1)/T]$, where the energy of the system is changed from E_1 to $E_2 (> E_1)$. As the temperature parameter T decreases slowly, the probability P becomes small. Then we may reach the global minimum of the function. In the following, we show how the method works, with a simple example.

2.2.2 Illustration of annealing method

We illustrate the annealing method applied to the traveling salesman problem. The N points are provided as shown in Fig.4, where a number of each point describes the initial order $i = 1, \ldots, N$, $N = 10$ in Fig.4. Each point locates at (x_i, y_i) and the solid line in the figure represents the initial route of the salesman. An arrangement is defined as a permutation of the number $1, \ldots, N$, interpreted as the ordering in which the points are visited.

The initial order is rearranged as follows. We randomly choose a segment from the initial route for the rearrangement. For example, in Fig.5, the segment of the route is chosen as the red line, where n_1 is the beginning of the segment and n_2 the end of the segment. Here, this segment is named n_1-n_2. We introduce an objective function E to estimate a degree of the optimization. This function can be defined as various forms according to considering cases. In our problem, the objective function is just given as the total length of the route,

$$E = \sum_{i=1}^{N} L(i, i+1), \tag{3}$$

where the point $i = N + 1$ is identified with the point $i = 1$, and $L(j, k)$ is defined to represent a path-length between a point j and a point k, i.e.,

$$L(j, k) := \sqrt{(x_j - x_k)^2 + (y_j - y_k)^2}. \tag{4}$$

For finding the solution of the problem, the function E should be minimized. In the method, we rearrange the order of the points according to the following two ways, *reversal* or *transplant*, which have the same probability.

The reversal operation is that the segment is removed and replaced with the same points in the opposite order. As shown in Fig.6, we reverse the segment n_1-n_2, i.e., we connect n_1 to n_4, and n_2 to n_3. In the figure, blue lines represent new paths after reversing the segment. We then introduce the cost of the reversal operation, $C_{\rm rev}$, defined by the difference between the total lengths of the route before and after the reversal operation, i.e., $C_{\rm rev} = E_{\rm after} - E_{\rm before}$. In the case of Fig.6, considering only changing paths, the cost of the reversal is

$$\begin{aligned} C_{\rm rev} &= \Big[L(2,7) + L(3,8)\Big] \\ &- \Big[L(2,3) + L(7,8)\Big]. \end{aligned} \tag{5}$$

The other way of rearranging the order of the points is given by the transplant operation. The operation is that the segment is removed and transplanted between two neighboring points which are randomly chosen from the points not on the segment. In Fig.7, the destination path of the transplant, n_3-n_4, is chosen. We transplant the segment n_1-n_2 into the destination path n_3-n_4, and close the route. In the figure, dashed-lines represent the old paths which are replaced by the blue paths after the transplant of the segment n_1-n_2 . The cost of the transplant operation, $C_{\rm tr}$, is given as

$$\begin{aligned} C_{\rm tr} &= \Big[L(2,8) + L(9,7) + L(3,10)\Big] \\ &- \Big[L(2,3) + L(7,8) + L(9,10)\Big]. \end{aligned} \tag{6}$$

After estimating the cost of the reversal or transplant operation, we actually adopt the rearrangement according to the probability P_A based on the Metropolis algorithm [24], where P_A is defined by the cost C and the temperature T,

$$P_A := \begin{cases} 1 & \text{for } C \le 0 \\ \exp(-C/T) & \text{for } C > 0 \end{cases}. \tag{7}$$

By the above operations, the *annealing*, i.e., escapade with the Boltzmann probability distribution $P(E)$ in Eq.(2), is executed.

We proceed the above steps, i.e., the repetition of the rearrangements and the annealing operations, according to an annealing schedule which controls a procedure how to reduce the temperature parameter T [23]. When efforts to reduce the total path-length E become sufficiently discouraging, the all calculation steps are stopped.

2.2.3 Demonstration and application of annealing method

We demonstrate the annealing method with an example of the traveling salesman problem. As shown

in Fig.8, an initial set of 30 random points is given, where the number means the initial order in which the points are visited, and the solid lines represent the initial route of the salesman. The total length of the initial route is calculated as $E_{\rm initial} = 18.16521$. The results of the simple method searching the nearest neighbor point and the simulated annealing method are shown in Figs.9 and 10, respectively. Each total length of the route is calculated as $E_{\rm nearest} = 4.994745$ and $E_{\rm anneal} = 4.546217$. Using the simulated annealing method, we obtain the better solution for the optimization of cyclical itinerary. This means that in the simple method, the system is trapped in a local minimum of the total length E, as shown in Fig.3, because of the no-good choice of the initial starting point. Therefore, even if the simple method does not work well as such a situation, we have alternative way, i.e., the simulated annealing method, to obtain the solution of the traveling salesman problem.

We apply the annealing method to order the Poincaré points of a field line. Specifically, we regard that the route connecting the points, which is obtained by using the annealing method, is the closed curve of a poloidal cross section of a magnetic flux-surface. Note that the minimum of E does not always guarantee to identify a flux-surface; in general, when the total number of the points is small, there are a lot of possible routes and the shortest route does not always express the true curve of the flux-surface. If the number of the points is sufficiently large, then the flux-surface is usually identified by the minimum of E.

As shown in Fig.11(a), the simple method searching the nearest neighbors often fails the ordering. Of course, if the number of the points becomes extremely large, then the simple method may succeed to obtain the flux-surface, but it is very time consuming. As shown in Fig.11(b), the annealing method can find the flux-surface with the comparable computing time to the case of Fig.11(a). Therefore, the annealing method enables us to obtain a flux-surface in realistic calculation time. Note that it is difficult to identify a rational surface by using the methods introduced here. In such a case, we define the rational surface by interpolating from neighbor irrational surfaces; see the part III of Fig.1.

2.3 Calculation of toroidal fluxes

In the last part of the developed technique, we calculate a value of toroidal magnetic flux Ψ_T and give the label `TFLUX` to the flux-surface. In the following, we consider the case of Ψ_A in Fig.2. As shown in the figure, we assign square areas ΔS_i to each grid-point (x_i, y_i) which is included in the interior region S_A on a poloidal cross section. Note that the accuracy of the calculation depends on the number of the grids. Convergence of the calculation will be discussed in Sec.2.4. The toroidal flux for the point A in Fig.2, for example, is written as

$$\Psi_T = \int_{S_A} B_\varphi \, dS, \tag{8}$$

where B_φ is the toroidal component of the magnetic field $\boldsymbol{B}$. A value of the magnetic field in an area ΔS_i is acted as substituted by the value at a grid-point (x_i, y_i), $\boldsymbol{B}^{(i)}$. We denote the toroidal component of $\boldsymbol{B}^{(i)}$ by $B_\varphi^{(i)}$. Thus we numerically proceed the calculation of toroidal flux by the sum of $B_\varphi^{(i)} \Delta S_i$,

$$\frac{\Psi_T}{\Psi_N} \simeq \frac{\sum_{(x_i,y_i)\in S_A} B_\varphi^{(i)} \Delta S_i}{\Psi_N} \equiv \texttt{TFLUX}, \tag{9}$$

where Ψ_N is the normalization and `TFLUX` is the label denoting the value of the toroidal flux. Of course, we can improve the integration scheme more precisely, although we use the above simple scheme.

If an evaluation point locates on a rational surface or an invisibly thin island, we calculate the toroidal fluxes at the neighbor points of the original point, and interpolate into the original point from the values at the neighbor points, as mentioned in the part III of Fig.1.

2.4 Numerical results

We confirm the convergence of calculating the toroidal flux according to the number of the grids ΔS_i. In Fig.12, our result is compared with analytic value of Ψ_T at the minor radius $r = 0.5$ m in the magnetic field of a simple tokamak configuration given as

$$\begin{aligned} B_R &= -\frac{B_0 R_0}{q}\frac{Z}{R^2}, \\ B_\varphi &= -B_0 R_0 \frac{1}{R}, \\ B_Z &= \frac{B_0 R_0}{q}\frac{(R-R_0)}{R^2}, \end{aligned} \tag{10}$$

in terms of the cylindrical coordinate system, (R, φ, Z), where B_0 is the strength of the magnetic field at the magnetic axis, R_0 the major radius of the axis, and q a safety factor. In Fig.12, $B_0 = 3$ T and $R_0 = 3.6$ m. From this figure, we can see that the relative error becomes small as increasing the number of the grids. The relative error does not significantly depend on the choice of a flux-surface except a rational surface.

We show the results for labeling the magnetic flux-surfaces in some magnetic field configurations. In Fig.13, we label the flux-surfaces on a poloidal section in a magnetic configuration given by adding an $m/n = 1/1$ magnetic island to the simple tokamak configuration, which is called the test configuration in this paper. The label of the regions of the magnetic field structure `IREGION` and the label of toroidal fluxes `TFLUX` are indicated by colors and their hues, respectively. Here, we consider the success rate of ordering the Poincaré points by the simple method. The rate is

proportional to the number of the flux-surfaces identified successfully, i.e., there are no crossing paths in the ordering and the points do not locate on a rational surface or an invisibly thin island. Table 1 shows the success rates of the simple method in the $m/n = 1/1$ magnetic island of the test configuration. From the table, we see that as the number of the points increases, the rate for the simple method approaches to 100 %, while the rate for the developed method is always 100 % for the all cases in the table. As shown in Fig.14, when the number of the points is small, the simple method often fails, because there is a case where the path-length in the true curve $L(i, j)$ is larger than the path-length in the wrong curve $L(i, k)$, i.e., $L(i, j) > L(i, k)$. Thus the simple method selects a wrong point, as shown in Fig.14. We should note that there exist some rational surfaces and invisibly thin islands in the configuration. When we encounter the points on a rational surface or an invisibly thin island, we interpolate the label of the surface from the neighboring irrational surfaces; see the part III of Fig.1.

Finally, figure 15 shows a result for the LHD vacuum configuration with the $m/n = 1/1$ island, where the vacuum magnetic field is calculated by using the Biot-Savart low [25–27]. In this figure, the green line represents the outside region which is very narrow, then magnetic flux-surfaces in the exterior of the line are not visible under the calculation accuracy. We have succeeded in labeling the magnetic flux-surfaces in the configuration with the island.

3 Summary

The labeling of magnetic flux-surfaces is needed for transport analysis in non-axisymmetric magnetic field configurations with magnetic islands. Frequently, it is not easy to label the flux-surfaces because of their complexity. We have developed the computational technique for labeling the magnetic flux-surfaces by applying the simulated annealing method. This is the algorithm to find the global extremum. Our problem is the ordering of the Poincaré points of field lines on a poloidal cross section to identify the closed magnetic flux-surfaces. In the developed technique, we label the flux-surfaces by two labels describing the regions of the magnetic field structure (`IREGION`), and the values of the toroidal magnetic fluxes (`TFLUX`). Of course, a magnetic coordinate system can be locally constructed on the island region by using the techniques of the present paper and Refs. [15–18].

Using the technique developed here, the flux-surface average can be obtained wherever closed flux-surfaces exist; for example, the flux-surface average of a function $\Phi(\boldsymbol{x})$ is given as

$$\langle \Phi(\boldsymbol{x}) \rangle \simeq \frac{1}{\Delta V} \iiint_{\Delta V} \Phi(\boldsymbol{x}) d^3x, \tag{11}$$

where ΔV is the volume of a small shell which lies between two neighboring flux-surfaces given by the developed technique. Note that in an ergodic region (`IREGION = 2`), the average is given as

$$\langle \Phi(\boldsymbol{x}) \rangle \simeq \frac{1}{V_2} \iiint_{V_2} \Phi(\boldsymbol{x}) d^3x, \tag{12}$$

where V_2 is the total volume of the ergodic region assumed to be narrow. The average may be useful to analyze the transport phenomena in terms of the neoclassical transport theory. The neoclassical transport analysis is frequently carried out on magnetic coordinates [28–31]. However, in an LHD equilibrium having the $m/n = 1/1$ island, there does not exist a magnetic coordinate system along the flux-surfaces in both the core and island regions. Therefore, we are developing a δf-transport simulation code based on computational techniques without magnetic coordinates [32–34]. The results of the transport analysis in/around the island region will be reported near future.

Acknowledgments

This work is performed with the support and under the auspices of the NIFS Collaborative Research Program NIFS05KNXN039, NIFS00KTAT002 and NIFS04KLDD001.

[1] S. Hamada, Nucl. Fusion **2**, 23 (1962).
[2] A. H. Boozer, Phys. Fluids **23**, 904 (1980).
[3] N. Nakajima, J. Todoroki and M. Okamoto, Kakuyugo Kenkyu **68**, 395 (1992).
[4] H. Grad, Phys. Fluids **10**, 137 (1967).
[5] T. Hayashi, *Theory of Fusion Plasmas* (Bologna, Società Italiana di Fisica, 1989) p.11.
[6] K. Harafuji, T. Hayashi and T. Sato, J. Comput. Phys. **81**, 169 (1989).
[7] R. Kanno, T. Hayashi and M. Okamoto, Nucl. Fusion **45**, 588 (2005).
[8] S. R. Hudson and R. L. Dewar, Phys. Lett. A **226**, 85 (1997).
[9] R. L. Dewar, S. R. Hudson and P. F. Price, Phys. Lett. A **194**, 49 (1998).
[10] J. Todoroki, J. Phys. Soc. Jpn. **58**, 3979 (1989).
[11] J. Todoroki, J. Phys. Soc. Jpn. **63**, 2168 (1994).
[12] M. Kurata and J. Todoroki, J. Plasma Fusion Res. SERIES **1**, 491 (1998).
[13] K. Ida, N. Ohyabu, T. Morisaki *et al.*, Phys. Rev. Lett. **88**, 015002 (2002).
[14] K. Ida, S. Inagaki, N. Tamura *et al.*, Nucl. Fusion **44**, 290 (2004).
[15] G. Kuo-Petravic, A. H. Boozer, J. A. Rome and R. H. Fowler, J. Comput. Phys. **51**, 261 (1983).
[16] J. A. Rome, J. Comput. Phys. **82**, 348 (1989).
[17] P. H. Fowler, R. N. Morris, J. A. Rome and K. Hanatani, Nuclear Fusion **30**, 997 (1990).
[18] H. Kikuchi, H. Ueno, M. Aizawa *et al.*, *Proceedings of the First International Toki Conference on Plasma Physics and Controlled Nuclear Fusion* (Toki, National Institute for Fusion Science, 1990) p.183.
[19] S. Kirkpatrick, C. D. Gelatt and M. P. Vecchi, Science **220**, 671 (1983).
[20] V. Černý, J. Optim. Theory Appl. **45**, 41 (1985).

[21] E. L. Lawler, J. K. Lenstra, A. H. G. Rinnooy Kan and D. B. Shmoys (Ed), *The Traveling Salesman Problem: A Guided Tour of Combinatorial Optimization* (Eastbourne, John Wiley & Sons Ltd, 1985).
[22] C. K. Koelbel, D. B. Loveman, R. S. Schreiber, G. L. Steele Jr. and M. E. Zosel, *The High Performance Fortran Handbook* (Cambridge Mass., MIT Press, 1993).
[23] W. H. Press, B. P. Flannery, S. A. Teukolsky and W. T. Vetterling, *Numerical Recipes in C* (New York, Cambridge University Press, 1986).
[24] N. Metropolis, A. Rosenbluth, M. Rosenbluth, A. Teller and E. Teller, J. Chem. Phys. **21**, 1087 (1953).
[25] J. Todoroki, Kakuyugo Kenkyu **57**, 318 (1987) [in Japanese].
[26] J. Todoroki, Kakuyugo Kenkyu **63**, 271 (1990) [in Japanese].
[27] J. Todoroki, Jpn. J. Appl. Phys. **43**, 1209 (2004).
[28] W. X. Wang, N. Nakajima, M. Okamoto and S. Murakami, Plasma Phys. Control. Fusion **41**, 1091 (1999).
[29] M. Okamoto, N. Nakajima, S. Satake and W. X. Wang, J. Plasma Fusion Res. **78**, 1344 (2002).
[30] S. Satake, M. Okamoto, N. Nakajima, H. Sugama and M. Yokoyama, Plasma Fusion Res. **1**, 002 (2006).
[31] P. Helander and D. J. Sigmar, *Collisional Transport in Magnetized Plasmas* (Cambridge, Cambridge University Press, 2002).
[32] R. Kanno, S. Jimbo, H. Takamaru and M. Okamoto, J. Plasma Fusion Res. SERIES **6**, 527 (2004).
[33] S. Jimbo, R. Kanno, H. Takamaru and M. Okamoto, J. Plasma Fusion Res. **80**, 649 (2004).
[34] S. Jimbo, R. Kanno, H. Takamaru, S. Satake and M. Okamoto, Nucl. Fusion **45**, 1534 (2005).

Table 1 The success rate of the simple method ordering the Poincaré points. The result is obtained in the $m/n = 1/1$ island in the test configuration. On the other hand, the developed method always successes.

Number of points	Success rate (%)
50	3.0
100	46.0
200	78.0
500	93.0

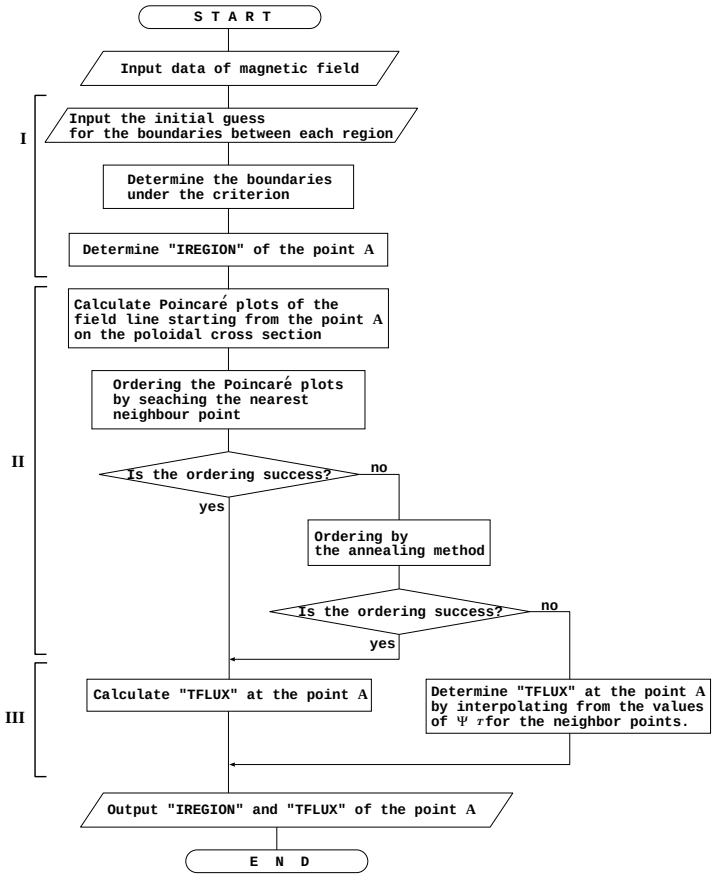

Fig. 1 Flowchart of the developed technique. The chart describes the procedure labeling a flux-surface which includes an evaluation point A. This technique is grouped into three parts: I) classification of regions, II) ordering Poincaré points, and III) calculation of toroidal magnetic flux, where `IREGION` is a label of the regions and `TFLUX` is a value of the toroidal flux.

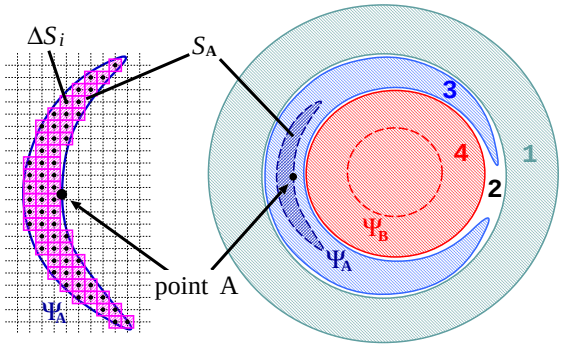

Fig. 2 Classification of the regions (right-hand) and illustration of calculating toroidal magnetic flux (left-hand). We classify the regions into four parts: outside, ergodic, island, and core regions by the label `IREGION` = 1, 2, 3, and 4, respectively. There does not exist a magnetic coordinate system along both the closed magnetic flux-surfaces, Ψ_A and Ψ_B. For calculating the toroidal flux `TFLUX` at the evaluation point A, we sum the toroidal fluxes $B_\varphi^{(i)}\Delta S_i$ over the interior region S_A of Ψ_A.

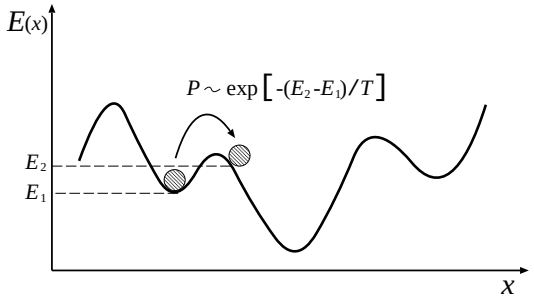

Fig. 3 Escapade from a local minimum. When the system is trapped in a local minimum E_1, it can escape from there, according to the probability $P \sim \exp[-(E_2 - E_1)/T]$.

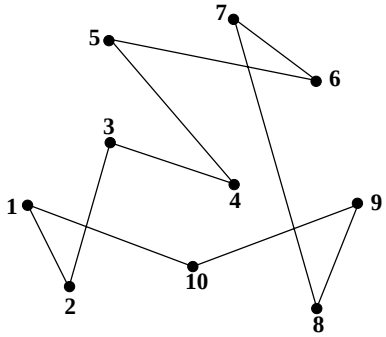

Fig. 4 The initial route of the traveling salesman problem. The numbers describe the initial order.

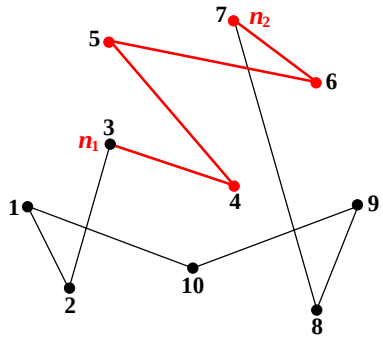

Fig. 5 The choice of the segment for the rearrangement. In this case, the segment n_1-n_2 indicated by the red line is the target for the rearrangement operations, i.e., *reversal* and *transplant*.

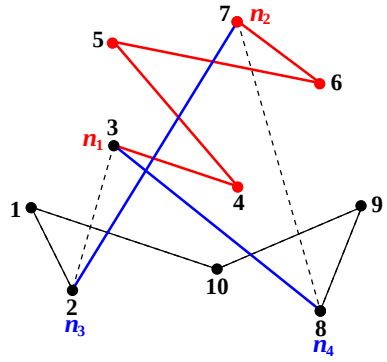

Fig. 6 Reversal of the segment n_1-n_2. In the reversal operation, the segment n_1-n_2 is reversed; i.e., the beginning point n_1 of the segment is connected to the point n_4, and the end point n_2 to the point n_3. Dashed lines represent the old paths before the reversal operation.

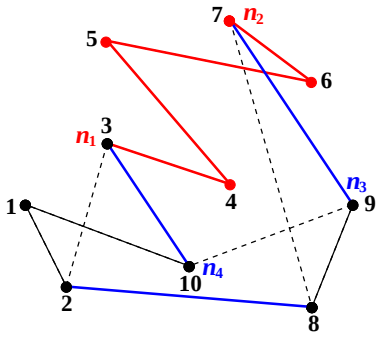

Fig. 7 Transplant of the segment n_1-n_2. In the transplant operation, the segment n_1-n_2 is transplanted into n_3-n_4 which is randomly chosen; i.e., the beginning point n_1 is connected to n_4, and the end point n_2 to n_3. The point 2 has to be connected to the point 8 in order to close the route. Blue lines represent new paths of the route, and dashed lines represent the old paths before the transplant operation. By repeating the transplant operation (this figure) and the reversal operation (Fig.6), the rearrangements of ordering the points are executed.

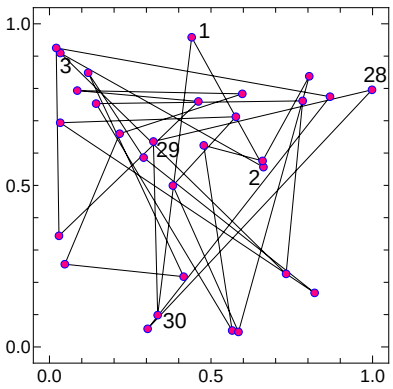

Fig. 8 The initial set of 30 points. The numbers describe the initial order and the solid line represents the initial route. The total length of the initial route is $E_{\mathrm{initial}} = 18.16521$.

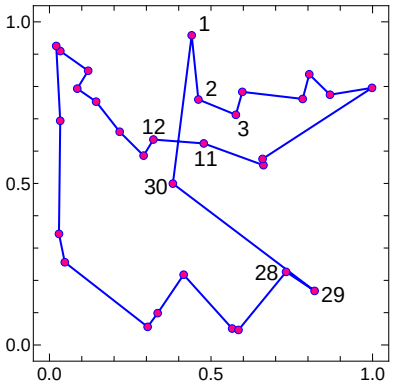

Fig. 9 The result given by the simple method searching the nearest neighbor point. The ordering fails, because the path from the point 30 to the point 1 crosses the path from 11 to 12. The total length of the route is $E_{\mathrm{nearest}} = 4.994745$.

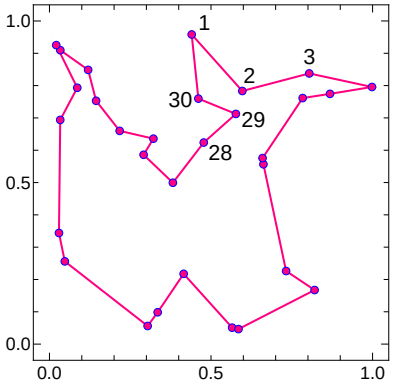

Fig. 10 The result given by the simulated annealing method. The ordering succeeds, because all paths from a point i to a point $i+1$ do not cross each other, where $i = 1, 2, \ldots, 30$, and the point 31 is identified the point 1. The solid line may be a better minimum solution of the total length of the route. In fact, the total length is $E_{\mathrm{anneal}} = 4.546217$, which is less than the result of the simple method in Fig.9.

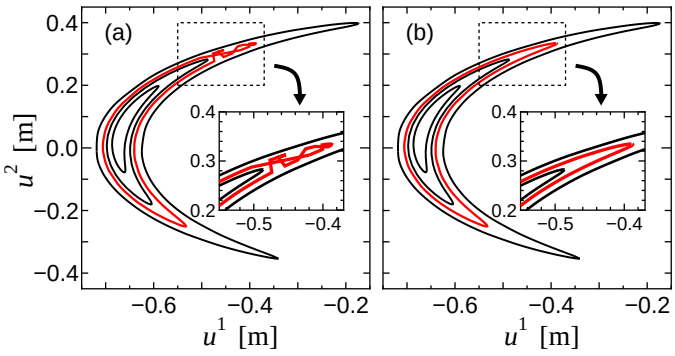

Fig. 11 Comparison between the results of two ordering methods, i.e., the simple method and the simulated annealing method, in an LHD configuration with an $m/n = 1/1$ island. The ordering by the simple method is unsuccessful; see the red line in figure (a). On the other hand, the simulated annealing method succeeds; see figure (b).

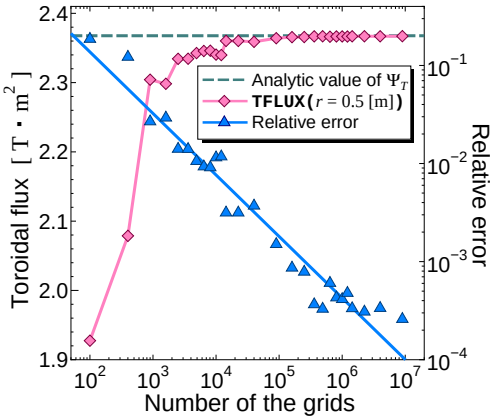

Fig. 12 Convergence of the calculation of Ψ_T at $r = 0.5$ m for the simple tokamak configuration. The blue line is given by the method of least squares.

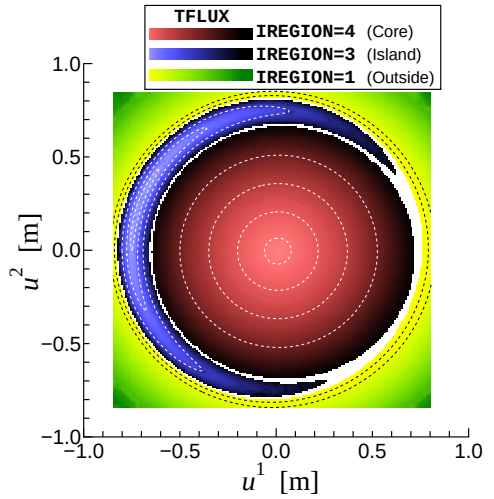

Fig. 13 The label of the magnetic flux-surfaces in the test configuration on a poloidal section, where `IREGION` and `TFLUX` are indicated by colors and their hues, respectively.

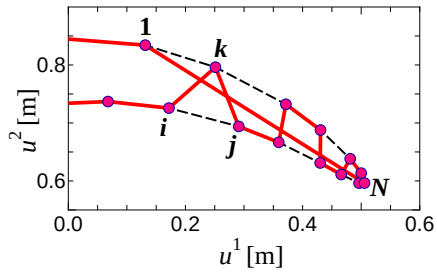

Fig. 14 A result of the simple method ordering the Poincaré points in the test configuration shown in Fig.13. The Red line represents failure connections of each point and the dashed line represents the true solution. Because $L(i,j) > L(i,k)$, the ordering fails. Note that the point N has to be connected to the point 1 in order to close the curve.

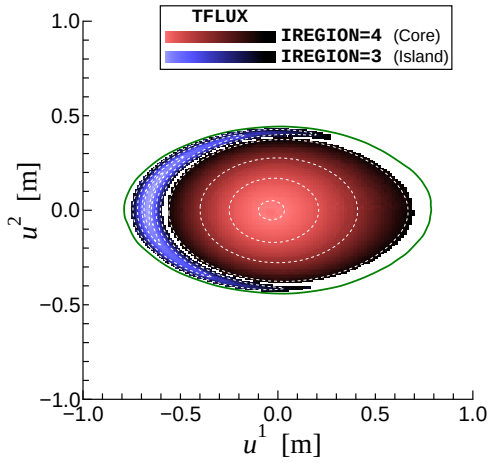

Fig. 15 The label of the magnetic flux-surfaces in the LHD configuration with the $m/n = 1/1$ island on a poloidal cross section. The labels, `IREGION` and `TFLUX`, are indicated by colors and their hues, respectively. The green line represents the outside region which is very narrow, and the flux-surfaces in the exterior of the line are not visible under the calculation accuracy.